The Effect of Bone Marrow Stimulation for Cartilage Repair on the Subchondral Bone Plate

Simone Birkebæk Elmholt[1] , Kris Chadwick Hede[1] ,
Bjørn Borsøe Christensen[2] , Jesper Skovhus Thomsen[3] ,
and Martin Lind[1]

Abstract

Purpose. To investigate the effect of bone-marrow stimulation (BMS) on subchondral bone plate morphology and remodeling compared to untreated subchondral bone in a validated minipig model.

Methods. Three Göttingen minipigs received BMS with drilling as treatment for two chondral defects in each knee. The animals were euthanized after six months. Follow-up consisted of a histological semiquantitative evaluation using a novel subchondral bone scoring system and micro computed tomography (μCT) of the BMS subchondral bone. The histological and microstructural properties of the BMS-treated subchondral bone were compared to that of the adjacent healthy subchondral bone.

Results. The μCT analysis showed that subchondral bone treated with BMS had significantly higher connectivity density compared to adjacent untreated subchondral bone (26 1/mm^3 vs. 21 1/mm^3, $P = 0.048$). This was the only microstructural parameter showing a significant difference. The histological semiquantitative score differed significantly between the subchondral bone treated with BMS and the adjacent untreated subchondral (8.0 vs. 10 $P = < 0.001$). Surface irregularities were seen in 43% and bone overgrowth in 27% of the histological sections. Only sparse formation of bone cysts was detected (1%).

Conclusions. BMS with drilling does not cause extensive changes to the subchondral bone microarchitecture. Furthermore, the morphology of BMS subchondral bone resembled that of untreated subchondral bone with almost no formation of bone cyst, but some surface irregularities and bone overgrowth.

Introduction

Cartilage injuries are a significant risk factor for developing early onset osteoarthritis due to the lack of spontaneous healing capacity of the articular cartilage.[1] Therefore, injuries to the cartilage leads to tissue deterioration, functional impairment, and joint pain—and if left untreated—these will progress to early onset osteoarthritis.[2,3] The most common treatment option for cartilage injuries is bone-marrow stimulation (BMS). The most popular BMS techniques is the subchondral drilling technique developed by K.H. Pridie[4] and the microfracture technique.[5] Today, the BMS techniques are considered first-line treatments.[6,7] The objective of BMS is to create canals in the subchondral bone to the underlying bone marrow, either by use of a drill[4] (subchondral drilling) or an awl[8] (microfracture). This facilitates recruitment of blood and bone marrow-derived mesenchymal stem cells (MSC) to the cartilage injury site, where they elicit a repair response. The subsequent proliferation and differentiation of the MSC's

at the injury site fills the cartilage defect area with repair tissue. The repair tissue mostly consists of fibrocartilage, which has inferior properties compared to the native hyaline cartilage.[9] However, how the canals formed during BMS affects the morphology and remodeling of the subchondral bone plate is not well established. Chen *et al.* investigated the subchondral bone structure after treatment with either microfracture or drilling 3 months postoperatively in a rabbit

[1]Department of Orthopaedics, Aarhus University Hospital, Aarhus, Denmark
[2]Department of Orthopaedics, Horsens Regional Hospital, Horsens, Denmark
[3]Department of Biomedicine, Aarhus University, Aarhus, Denmark

Corresponding Author:
Simone Birkebæk Elmholt, Department of Orthopaedics, Aarhus University Hospital, Palle Juul-Jensens Boulevard 99, 8200 Aarhus N, Denmark.
Email: elmholt94@live.dk

model.[10] They showed that the treatment increased the connectivity density of the subchondral bone compared with intact controls using micro computed tomography (μCT). Chen *et al.* also observed "incomplete fill, cyst formation, bone overgrowth, and poor bone integration" in the subchondral bone.[10] Orth *et al.* investigated the effect of drilling the subchondral bone 6 months postoperatively in sheep.[11] They found presence of subchondral bone cyst and intralesional osteophytes in 74% of the specimens. Their μCT investigation showed decreased bone mineral density, bone volume fraction, and cortical thickness compared with the adjacent healthy subchondral bone.[11]

However, these studies were performed in either rabbits or sheep, which both have several translational issues. Rabbits possess better endogenous healing capacity[12] and have less cancellous bone than humans,[13] while sheep have a denser and stronger trabecular bone than humans.[14] In order to overcome these translational issues, minipigs can be employed. Minipigs offer a model with closer resemblance to the human setting.[15] Minipig bone have several similarities to human bone, including bone mineral density, healing capacity, joint size, remodeling rate, and bone morphology. The downside of minipigs is that they are more expensive and are more difficult to handle compared to smaller animals.[16]

Due to the sparse research on the effects of BMS on subchondral bone plate morphology and remodeling, the aim of this study was to investigate the effects of subchondral drilling 6 months postoperatively in a validated minipig model. The hypothesis was that the subchondral bone volume fraction (BV/TV) would increase after treatment with BMS compared with that of the adjacent untreated subchondral bone.

Materials and Methods

Experimental Design

Three skeletally mature male Göttingen minipigs (weight 38.4 kg, range: 36.4-43.6 kg; age 19.4 months, range: 18.9-21.1 months) were treated with BMS as previously described.[17] Two cylindrical chondral defects were created in the trochlea of each knee with a diameter of 6 mm yielding a total of 12 defects. One defect was created in the medial trochlear facet and one in the lateral trochlear facet. Then, all defects were treated with BMS using the Pridie drilling technique.[4]

The study was conducted according to the Danish Law on Animal Experimentation and approved by the Danish Ministry of Justice Ethical Committee (J.nr. 2017-15-0201-01343).

Surgery

The animals were premedicated with Zoletil Mix 1 ml/10 kg (tiletamin 2.5 mg/ml, zolazepam 2.5 mg/ml, torbugesic

0.5 mg/ml, ketaminol 2.5 mg/ml, and rompun 2.5 mg/ml; Virbac, DK). General anesthesia and local analgesia were achieved with Etomidate (hypnomidate, 0.25 ml/kg; Janssen Pharmaceuticals), sevoflurane (3%; AbbVie), fentanyl (0.175 ml/kg/h; Hameln Pharmaceuticals), and Lidocaine (Xylocaine 10 ml, 20 mg/ml; AstraZeneca). Preoperative prophylactic antibiotics were used (penicillin procaine, 0.03 ml/kg; Ceva Sante Animale, 33500 Libourne, France).

Access to the knee joint was gained through the patellar ligament. The trochlea was exposed, and 2 chondral defects with a diameter of 6 mm were created using a skin biopsy punch and a curette. One defect was made in the distal, medial trochlea, while the other was made in the lateral trochlea, 0.5 to 1 cm proximal to the first defect. This was performed in all knees, and both defects in each knee were treated with the same method. The defects were thoroughly debrided using a curette, and the calcified cartilage layer was carefully removed in order not to damage the subchondral bone. The defects were treated with BMS by drilling 4 holes (depth 5 mm, diameter 1 mm) into the subchondral bone. Hand-drilling without irrigations was performed and bleeding form the bone marrow was observed.

After BMS by drilling, the patella ligament, the subcutaneous tissue, and the skin were sutured, and subcutaneous lidocaine was injected for pain management. Postoperatively, the animals were treated postoperatively with Finadyne 5% (Flunixin meglumin, 1.1 mg/kg, oral paste, Intervet, Denmark) for 5 days, and allowed weight bearing and full-range of motion. Trained animal keepers, supervised by a veterinarian, closely observed all animals thrice daily. After 6 months the animals were euthanized using Pentobarbital (0.4 ml/kg). Osteochondral blocks of 1 cm × 1 cm × 1 cm including the defect and adjacent healthy cartilage and subchondral bone were obtained for further analyses.[17]

Preparation of Specimens

The osteochondral blocks were dehydrated in ethanol of increasing concentration (70%–96%) at 4°C. Then they were cleared in isopropanol and xylene and embedded undecalcified in methyl methacrylate (MMA) at −20°C.[17]

μCT

The MMA embedded osteochondral blocks were scanned in a desktop μCT scanner (Scanco μCT 35; Scanco Medical, Brüttiselen, Switzerland) with an isotropic voxel size of 10 μm, X-ray voltage of 55 kV, current of 145 μA, and an integration time of 800 ms in high resolution mode (1000 projections/180°).

The trabecular bone was analyzed by drawing a 2-mm-high cylindrical volume of interest (VOI) with a diameter of 6 mm in the trabecular bone beneath the defect using a custom-made computer program running under Linux.[18] The

Table 1. Novel Semiquantitative Scoring System to Score Subchondral Bone Pathology Based on Five Parameters: "Subchondral Bone Plate Surface", "Resorption of Subchondral Bone", "Residual Drill Holes", "Bone Overgrowth" and "Bone Cysts".

Category	Parameters		Score	Total Score
Subchondral bone plate surface	Regular surface		2	2
	Irregular surface	Minor	1	
		Major	0	
Resorption of subchondral bone	Normal/near normal		2	2
	Yes	Minor	1	
		Major	0	
Residual drill holes	No		2	2
	Yes	1 drill hole	1	
		> 1 drill hole	0	
Bone overgrowth	None		2	2
	Minor		1	
	Major		0	
Bone cyst	None		2	2
	<3 mm		1	
	>3 mm		0	

VOI was imported into the software provided with the scanner (IPL version 6.5). The 3D data sets were low-pass filtered using a Gaussian filter ($\sigma = 1.3$, support = 2) in order to remove noise before segmentation with a fixed threshold filter (threshold = 510.3 mg HA/cm^3).

Analyses included bone volume fraction (BV/TV), trabecular thickness (Tb. Th), trabecular number (Tb.N), trabecular separation (Tb.Sp), connectivity density (CD), structure model index (SMI), tissue mineral density (TMD), and bone mineral density (BMD).[17]

Histological Evaluation

Half of each of the 12 blocks containing the cartilage defects and underlying subchondral bone were cut into 7-μm-thick sections by using a hard tissue microtome (Reichert Jung Polycut), stained with hematoxylin and eosin, and mounted on microscope slides. This yielded a total of 108 sections (9 sections per sample) for the semiquantitative scoring.

Semiquantitative Scoring

The subchondral bone repair was scored using a novel scoring system made for scoring subchondral bone after treatment with BMS (**Table 1**). The score included the following parameters: "subchondral bone plate surface," "resorption of subchondral bone," "residual drill holes," "bone cysts," and "bone overgrowth." All parameters received a score of either 0, 1, or 2 with 0 as the lowest and 2 as the highest score so a score of 10 represented normal subchondral bone. Depressions in the subchondral bone plate larger than 1 mm were considered to be remaining drill holes. The subchondral bone plate was considered irregular if the transition between the subchondral bone plate and the defect site

could not be identified or if there were residual drill holes. Irregularities were further graded as minor or major according to the extent of the irregularity. Bone resorption was defined as areas where the subchondral bone plate was not at the same level as the adjacent intact subchondral bone plate. Bone resorptions were further graded as minor or major according to the affected area. Bone overgrowth was defined as areas where the subchondral bone plate had grown into the cartilage. The bone overgrowth was further graded as minor or major according to the extent of the overgrowth. Bone cysts, if present, were graded according to their size (i.e., < 3 mm or > 3 mm).

The assessment was performed by one main observer and verified by two additional observers. Pearson correlation coefficients between the main observer and the two additional observers was $r = 0.66$ and $r = 0.75$, respectively.

Statistical Analysis

Sample size was determined by power analysis based on BV/TV as the primary endpoint. Based on recent studies we expected that BV/TV after subchondral drilling would be 0.39 and the BV/TV of the normal subchondral bone would be 0.25. Standard deviation (SD) for BV/TV was in previous studies 0.08. Power was set to 80%, $\alpha = 0.05$ and $\beta = 0.2$. With these assumptions 5 treatment units per study group was needed. The 6 units that were available were included, since the other 6 was lost in transport. Data from μCT were compared to adjacent healthy subchondral bone using unpaired *t*-tests. A *P*-value < 0.05 was considered significant.

A mean score was calculated for each parameter of the scoring system for the subchondral bone. The mean total score of subchondral bone was calculated and compared to

Table 2. µCT Data ± Standard Deviations and *P*-Value for BMS-Group and Control-Group.

Parameter	BMS	Controls	P Value
Bone volume fraction (BV/TV)	0.39 ± 0.082	0.36 ± 0.044	0.364
Connectivity density (CD) (1/mm^3)	**25.7 ± 2.74**	**21.4 ± 2.7**	**0.048**
Trabecular number (Tb N) (1/mm)	2.86 ± 0.24	2.85 ± 0.11	0.968
Trabecular thickness (Tb Th) (mm)	0.13 ± 0.023	0.11 ± 0.011	0.136
Trabecular spacing (Tb Sp) (mm)	0.32 ± 0.039	0.31 ± 0.016	0.737
Bone material density (BMD) (mg HA/cm^3)	401 ± 72.5	370 ± 43.2	0.397
Structure model index (SMI)	−1.15 ± 0.73	−0.93 ± 0.42	0.531
Tissue mineral density (TMD) (mg/cm^{-3})	837 ± 16.0	855 ± 17.4	0.103

BMS = bone marrow stimulation. The bold faced value refers to the only parameter that was statistically significant difference in the micro CT analysis.

Table 3. The Mean Scores of Each Parameter of the Twelve Defects Including the Mean Total Score. The Scores of Each Parameter Range from 0–2 and the Overall Score from 0–10, as Described in Table 1.

Sample Number	Subchondral Bone Plate Surface	Bone Resorption	Residual Drill Holes	Bone Overgrowth	Bone Cyst	Overall Score
No. 1	1.33	1.78	1.44	1.89	2	8.44
No. 2	2	1.0	1.44	1.89	2	8.44
No. 3	1.11	1.55	1.44	1.66	2	7.78
No. 4	1	1.88	1	2	2	7.88
No. 5	1.44	0.56	1.44	2	1.89	7.33
No. 6	1.86	1.86	1.86	1.43	2	9
No. 7	1.78	1	1.78	1.56	2	8.11
No. 8	1.89	1.78	1.89	1.56	2	9.11
No. 9	1.22	0.78	1.56	1.56	2	7.11
No. 10	1.25	1	1.38	1	2	6.63
No. 11	2	1.67	2	1.89	2	9.56
No. 12	0.17	0	2	2	2	6.17
Mean	1.42	1.24	1.65	1.69	1.99	7.99
SD	0.53	0.61	0.32	0.30	0.03	1.09

SD = standard deviation.

the maximum score resembling normal, healthy bone with an unpaired *t*-test. Statistical analysis was performed using Prism 8 (GraphPad Software, Inc.).

Results

µCT

Subchondral bone treated with BMS had a significantly higher connectivity density than control bone (26 1/mm^3 vs. 21 1/mm^3, $P = 0.048$), indicating that the trabecular bone network was more well connected in BMS bone compared to the control bone (**Table 2**). The other microstructural parameters assessed using µCT did not differ significantly between the two groups.

Semiquantitative Scoring

For each sample, 9 sections were scored using the subchondral scoring system. A few of the sections did not

include the cartilage defect area and were therefore not included in the assessment (in total, 8 sections were discarded leaving 100 sections for evaluation). The score of the 12 samples containing BMS subchondral bone was compared to the score of the control samples containing untreated subchondral bone. All control samples received a score of 10, as expected. The subchondral score differed significantly between normal subchondral bone and subchondral bone, which had been treated with BMS (10 ± 0.00 vs. 8.00 ± 1.05, $P = 0.00002$) (**Table 3**). Irregularity of the subchondral bone plate and subchondral bone resorption were the most pronounced subchondral bone changes seen. Ten out of the 12 samples showed irregularity of the subchondral bone plate, which was present in 43% of the sections. The most severe irregularities were seen in sample number 12 (mean = 0.17) (**Fig. 1A**). Bone cyst was a rare phenomenon and only occurred in 1 sample corresponding to 1% of the sections (**Fig. 1B**). Remains of the drill holes were seen in 9 out of the 12 samples
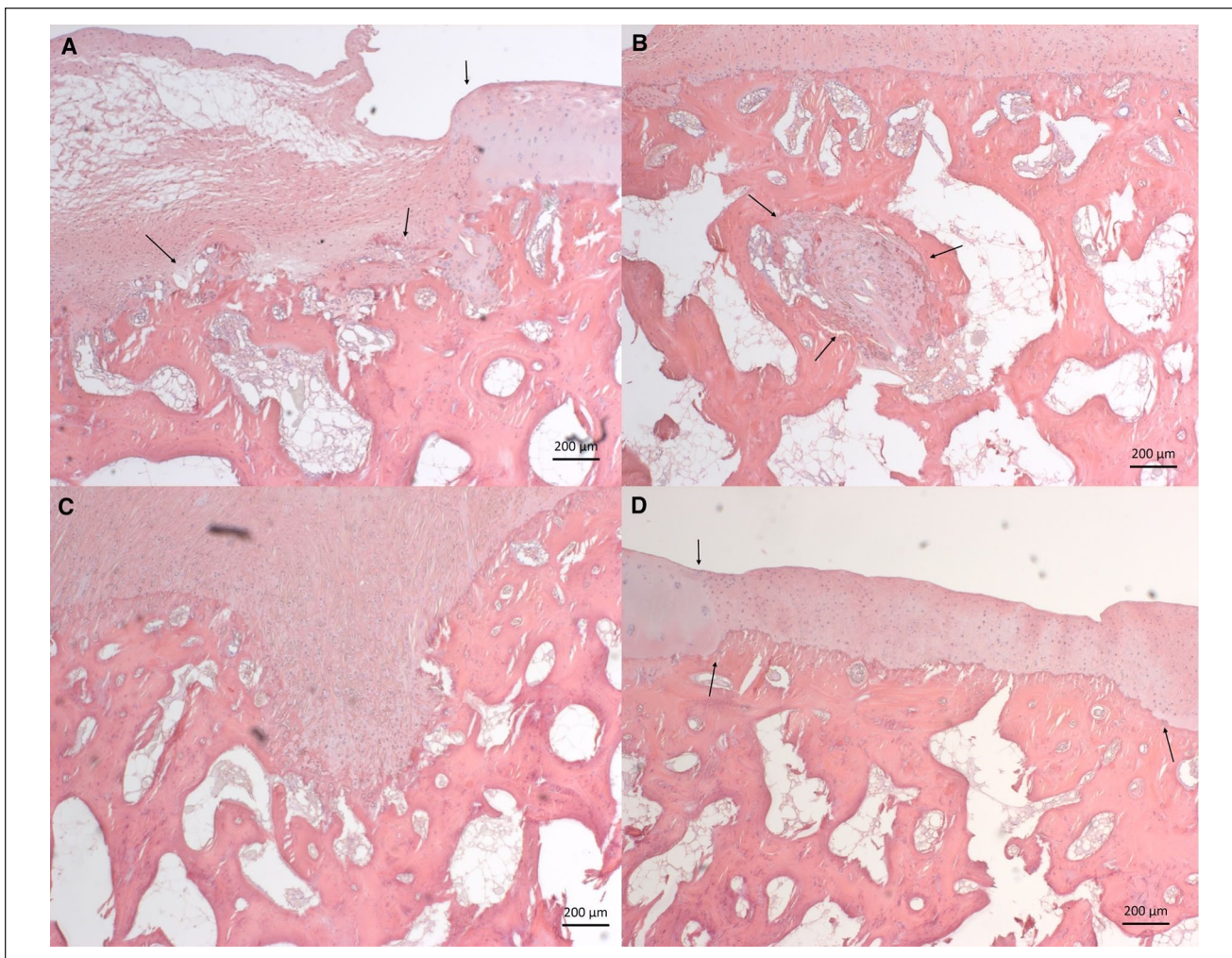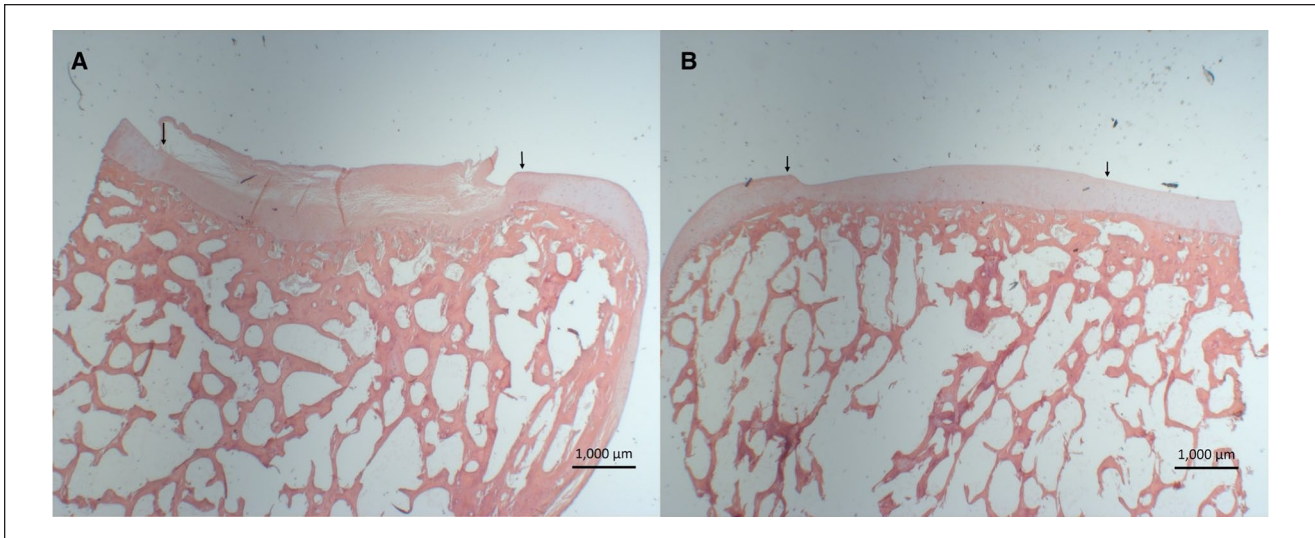
Figure 1. Hematoxylin eosin staining, scale bars: 200 μm. Defects treated with BMS. (**A**) Shows irregularity of the subchondral bone plate (top arrow marks the beginning of the defect). (**B**) Bone cyst marked by arrows. (**C**) Remaining drill hole in the subchondral bone plate. (**D**) Overgrowth in the subchondral bone plate marked by to arrows, top ar-row marks the beginning of the defect site. BMS = bone marrow stimulation.

corresponding to 31% of the sections. In most samples, the residual drill holes consisted of small depressions in the subchondral bone plate (**Fig. 1C**). Nine out of the 12 samples contained bone overgrowth corresponding to 27% of the sections. Sample number 6 had the worst case of bone overgrowth (mean = 1.43), which extended through most of the cartilage defect site (**Fig. 1D**). In most sections, bone overgrowth affected only minor parts of the cartilage defect site. Resorption was the parameter, which received the lowest mean score (**Table 2**). Resorption was seen in all of the 12 samples and in 46% of the slides with the lowest score seen in sample number 12 (mean = 0), which had bone resorption in all sections (**Fig. 2A**). The subchondral bone plate in sample number 11 had the highest resemblance to the adjacent normal subchondral bone with a total score of 10 in 5 out of the 9 sections (**Fig. 2B**). This

sample had only minor areas with bone resorption in 3 sections, and bone overgrowth in only 1 section.

Discussion

The main finding of this present study was that treatment with BMS had no substantial impact on the subchondral bone microarchitecture evaluated by μCT. We hypothesized that BMS would lead to a more compact subchondral trabecular bone. However, this was not the case as connectivity density was the only microstructural parameter that was statistically affected by BMS-treatment, resulting in not a denser but a more well connected trabecular bone network. Connectivity density is a measure of the connectedness of the trabecular network per unit volume and has been shown to have minor influence on the strength and elastic properties of normal

Figure 2. Hematoxylin eosin staining, scale bars: 1,000 μm. Defects treated with BMS. (**A**) Shows resorption of the subchondral bone plate covering the entire area under the defect. Defect area are marked by arrows. (**B**) Shows a section with a full score from sample number 11.

trabecular bone.[19,20] However, as suggested by Kabel *et al.*, this might differ in bone that is actively undergoing remodeling as is the case in the present study.[20]

The μCT findings are consistent with those of Chen *et al.*, who found an increased connectivity density in rabbits 3 months after treatment with BMS with the drilling technique.[10] Orth *et al.* investigated the effects of subchondral drilling to the subchondral bone after 6 months in an ovine model.[11] They found that the trabecular bone pattern factor decreased with drilling, and stated "trabecular bone pattern factor is an inverse index of connectivity" indicating that drilling increased connectivity. They also found that bone mineral density (BMD), bone volume fraction (BV/TV), and trabecular thickness (Tb. Th) were decreased in the subchondral bone that had been treated with drilling. The studies by Chen *et al.* and Eldracher *et al.* supports their findings of a decrease in bone volume fraction (BV/TV) in groups treated with BMS compared to controls.[10,21] Bone mineral density and bone volume fraction are strongly correlated with trabecular bone strength.[19] Since these parameters did not differ between BMS treated and control samples in this present study, it suggests that BMS did not affect the strength of the subchondral trabecular bone. Therefore, the findings of this present study do not support those of the above-mentioned studies. However, these studies are performed in sheep or rabbits and not in minipigs, which might explain the different outcome.

In the present study, BMS was performed using a slim drill with a width of 1 mm and a depth of 5 mm as previous studies have found that drilling deeper and with a narrower drill improves subchondral bone healing.[21-23] It has been suggested that the heat generated in the drilling process causes thermal necrosis to the adjacent subchondral bone and hereby impair the healing response. However, the study by Chen *et al.* found that bone surrounding the drilling holes remained morphologically intact with minimal osteocyte necrosis.[22] In the present study, hand-drilling was used to minimize heat induced bone trauma.

The histologic semiquantitative scoring of the subchondral bone plate of the BMS treated animals ranged from almost no remodeling to a more pronounced remodeling with substantial bone resorption. Bone resorption was the most affected parameter of the subchondral scoring system and was seen in almost half of the sections. Fisher *et al.* found a more pronounced bone remodeling when the cartilage injury was included in the cartilage-subchondral bone interface.[24] They showed that full-thickness cartilage defects, which involve the underlying subchondral bone, showed a more pronounced resorption than cartilage injuries that did not have contact to the underlying subchondral bone.[24] This may imply that the bone resorption and remodeling occur as a response to the subchondral bone injury generated by the BMS. In the present study, the pronounced bone resorption may indicate that the subchondral bone plate is still undergoing remodeling after a period of 6 months. Thus, it is possible that the repair and the normalization of the subchondral bone would have further developed with a longer follow-up period. Furthermore, the repair response in the subchondral bone might be affected by the lack of immobilization after surgery, which was not possible in the minipig model.[15]

In the present study, bone cysts were only seen in 1 section (1%) as opposed to the studies by Chen *et al.*, where bone cysts were present in all treated specimens,[10] and Orth

et. al. who found that BMS led to the formation of bone cyst in the subchondral bone in 63% of the specimens.[11] Interestingly, a more recent study from the same group showed no signs of subchondral bone cysts in any of their specimens.[21] They suggested that the inconsistency was due to topographical differences present in their ovine model.[25] It is not known whether a similar topographical difference exists in the minipig model. Cyst formation is associated with impaired joint function and pain as well as osteoarthritis.[26] Although remodeling had occurred, the histological score of the subchondral bone treated with BMS resembled the score of the adjacent subchondral bone with an overall mean score of 8 (10 being normal subchondral bone).

BMS has been used for cartilage repair for several decades. Follow-up studies with magnetic resonance imaging for patients treated with BMS using the microfracture technique have shown both intralesional osteophyte formations, due to subchondral bone overgrowth, and subchondral cyst formation to various degrees.[27-29] The subchondral bone alterations seen in these clinical studies cannot be explained by the findings of this pre-clinical study. In the present study, the subchondral bone treated with BMS with drilling had almost no cyst formation and very limited intralesional osteophyte formations as subchondral bone overgrowth was sparse.

This study has some limitations. The semiquantitative scoring of the subchondral bone plate was based on a novel subchondral scoring system, which has not yet been validated. This non-validated scoring was applied due to the lack of an existing validated method that focuses mainly on the subchondral bone instead of the cartilage defect. Furthermore, the semiquantitative score was based on only half of the BMS treated area, since only half of the samples were available. This was believed to be representative, but an evaluation of the entire BMS treated area may have changed the results. For instance, more cysts could be present, although the number of cysts would likely not have been substantially higher. Another limitation is that bone samples were evaluated at only 1 time point, so it was not possible to observe the long-term effects of BMS on the subchondral bone plate. The reason for studying a single time point only was mainly cost related.[17] However, the follow-up period of 6 months was either equal to or longer than those used in other studies.[10,11,21,22,30]

The strength of the study was that it was performed with a validated large animal model with good resemblance and translation to humans.[14,15,31] Furthermore, the subchondral bone was evaluated by both histology and μCT. Hence, the present study adds to the understanding of the effect of BMS on the subchondral bone.

In conclusion, BMS with drilling had little impact on subchondral remodeling and microstructure. Only small changes in surface irregularities and bone overgrowth as well as increased trabecular connectivity was found compared to the adjacent untreated subchondral bone.

Declaration of Conflicting Interests

The author(s) declared no potential conflicts of interest with respect to the research, authorship, and/or publication of this article.

Ethical Approval

The study was conducted according to the Danish Law on Animal Experimentation and approved by the Danish Ministry of Justice Ethical Committee (J.nr. 2017-15-0201-01343).

ORCID iDs

Simone Birkebæk Elmholt https://orcid.org/0000-0003-0445-5849
Kris Chadwick Hede https://orcid.org/0000-0002-3309-5320
Bjørn Borsøe Christensen https://orcid.org/0000-0002-3207-4536
Jesper Skovhus Thomsen https://orcid.org/0000-0001-9386-6679
Martin Lind https://orcid.org/0000-0002-7204-813X

References

1. Buckwalter JA, Mankin HJ. Articular cartilage: degeneration and osteoarthritis, repair, regeneration, and transplantation. Instr Course Lect. 1998;47:487-504.
2. Makris EA, Gomoll AH, Malizos KN, Hu JC, Athanasiou KA. Repair and tissue engineering techniques for articular cartilage. Nat Rev Rheumatol. 2015;11:21-34. doi:10.1038/nrrheum.2014.157.
3. Poulet B, Staines KA. New developments in osteoarthritis and cartilage biology. Curr Opin Pharmacol. 2016;28:8-13. doi:10.1016/j.coph.2016.02.009.
4. Müller B, Kohn D. [Indication for and performance of articular cartilage drilling using the Pridie method]. Orthopade. 1999;28(1):4-10. doi:10.1007/s001320050315.
5. Steadman JR, Rodkey WG, Briggs KK. Microfracture: its history and experience of the developing surgeon. Cartilage. 2010;1(2):78-86. doi:10.1177/1947603510365533.
6. Chimutengwende-Gordon M, Donaldson J, Bentley G. Current solutions for the treatment of chronic articular cartilage defects in the knee. EFORT Open Rev. 2020;5(3):156-63. doi:10.1302/2058-5241.5.190031.
7. Frank RM, Cotter EJ, Hannon CP, Harrast JJ, Cole BJ. Cartilage restoration surgery: incidence rates, complications, and trends as reported by the american board of orthopaedic surgery part II candidates. Arthroscopy. 2019;35(1):171-8. doi:10.1016/j.arthro.2018.08.028.
8. Steadman JR, Rodkey WG, Rodrigo JJ. Microfracture: surgical technique and rehabilitation to treat chondral defects. Clin

Orthop Relat Res. 2001;391:S362-9. doi:10.1097/00003086-200110001-00033.

9. Shapiro F, Koide S, Glimcher MJ. Cell origin and differentiation in the repair of full-thickness defects of articular cartilage. J Bone Joint Surg Am. 1993;75(4):532-53. doi:10.2106/00004623-199304000-00009.

10. Chen H, Chevrier A, Hoemann CD, Sun J, Ouyang W, Buschmann MD. Characterization of subchondral bone repair for marrow-stimulated chondral defects and its relationship to articular cartilage resurfacing. Am J Sports Med. 2011;39:1731-1740. doi:10.1177/0363546511403282.

11. Orth P, Goebel L, Wolfram U, Ong MF, Gräber S, Kohn D, et al. Effect of subchondral drilling on the microarchitecture of subchondral bone: analysis in a large animal model at 6 months. Am J Sports Med. 2012;40:828-36. doi:10.1177/0363546511430376.

12. Wei X, Gao J, Messner K. Maturation-dependent repair of untreated osteochondral defects in the rabbit knee joint. J Biomed Mater Res. 1997;34(1):63-72. doi:10.1002/(sici)1097-4636(199701)34:1<63::aid-jbm9>3.0.co;2-l.

13. Castañeda S, Largo R, Calvo E, Rodriguez-Salvanés F, Marcos ME, Díaz-Curiel M, et al. Bone mineral measurements of subchondral and trabecular bone in healthy and osteoporotic rabbits. Skeletal Radiol. 2006;35:34-41. doi:10.1007/s00256-005-0022-z.

14. Nafei A, Danielsen CC, Linde F, Hvid I. Properties of growing trabecular ovine bone. Part I: mechanical and physical properties. J Bone Joint Surg Br. 2000;82(6):910-20. doi:10.1302/0301-620x.82b6.9836.

15. Gotterbarm T, Breusch SJ, Schneider U, Jung M. The minipig model for experimental chondral and osteochondral defect repair in tissue engineering: retrospective analysis of 180 defects. Lab Anim. 2008;42(1):71-82. doi:10.1258/la.2007.06029e.

16. Wancket LM. Animal models for evaluation of bone implants and devices: comparative bone structure and common model uses. Vet Pathol. 2015;52(5):842-50. doi:10.1177/0300985815593124.

17. Hede K, Christensen BB, Olesen ML, Thomsen JS, Foldager CB, Lind MC. CARGEL Bioscaffold improves cartilage repair tissue after bone marrow stimulation in a minipig model. J Exp Orthop. 2020;7:26. doi:10.1186/s40634-020-00245-7.

18. Sikjaer T, Rejnmark L, Thomsen JS, Tietze A, Brüel A, Andersen G, et al. Changes in 3-dimensional bone structure indices in hypoparathyroid patients treated with PTH(1-84): a randomized controlled study. J Bone Miner Res. 2012;27(4):781-8. doi:10.1002/jbmr.1493.

19. Thomsen JS, Ebbesen EN, Mosekilde L. Predicting human vertebral bone strength by vertebral static histomorphometry. Bone. 2002;30(3):502-8. doi:10.1016/s8756-3282(01)00702-5.

20. Kabel J, Odgaard A, van Rietbergen B, Huiskes R. Connectivity and the elastic properties of cancellous bone. Bone. 1999;24:115-20. doi:10.1016/s8756-3282(98)00164-1.

21. Eldracher M, Orth P, Cucchiarini M, Pape D, Madry H. Small subchondral drill holes improve marrow stimulation of articular cartilage defects. Am J Sports Med. 2014;42(11):2741-50. doi:10.1177/0363546514547029.

22. Chen H, Sun J, Hoemann CD, Lascau-Coman V, Ouyang W, McKee MD, et al. Drilling and microfracture lead to different bone structure and necrosis during bone-marrow stimulation for cartilage repair. J Orthop Res. 2009; 27:1432-8. doi:10.1002/jor.20905.

23. Chen H, Hoemann CD, Sun J, Chevrier A, McKee MD, Shive MS, et al. Depth of subchondral perforation influences the outcome of bone marrow stimulation cartilage repair. J Orthop Res. 2011;29(8):1178-84. doi:10.1002/jor.21386.

24. Fisher MB, Belkin NS, Milby AH, Henning EA, Bostrom M, Kim M, et al. Cartilage repair and subchondral bone remodeling in response to focal lesions in a mini-pig model: implications for tissue engineering. Tissue Eng Part A. 2015; 21:850-60. doi:10.1089/ten.TEA.2014.0384.

25. Orth P, Meyer HL, Goebel L, Eldracher M, Ong MF, Cucchiarini M, et al. Improved repair of chondral and osteochondral defects in the ovine trochlea compared with the medial condyle. J Orthop Res. 2013;31(11):1772-9. doi:10.1002/jor.22418.

26. Gao L, Cucchiarini M, Madry H. Cyst formation in the subchondral bone following cartilage repair. Clin Transl Med. 2020;10(8): e248. doi:10.1002/ctm2.248.

27. Brown WE, Potter HG, Marx RG, Wickiewicz TL, Warren RF. Magnetic resonance imaging appearance of cartilage repair in the knee. Clin Orthop Relat Res. 2004;422:214-23. doi:10.1097/01.blo.0000129162.36302.4f.

28. Gudas R, Gudaite A, Pocius A, Gudiene A, Cekanauskas E, Monastyreckiene E, et al. Ten-year follow-up of a prospective, randomized clinical study of mosaic osteochondral autologous transplantation versus microfracture for the treatment of osteochondral defects in the knee joint of athletes. Am J Sports Med. 2012;40(11):2499-508. doi:10.1177/0363546512458763.

29. Mithoefer K, Williams RJ 3rd, Warren RF, Potter HG, Spock CR, Jones EC, et al. The microfracture technique for the treatment of articular cartilage lesions in the knee. A prospective cohort study. J Bone Joint Surg Am. 2005;87(9):1911-20. doi:10.2106/jbjs.D.02846.

30. Hayashi S, Nakasa T, Ishikawa M, Nakamae A, Miyaki S, Adachi N. Histological evaluation of early-phase changes in the osteochondral unit after microfracture in a full-thickness cartilage defect rat model. Am J Sports Med. 2018;46:3032-9. doi:10.1177/0363546518787287.

31. Christensen BB, Foldager CB, Olesen ML, Vingtoft L, Rölfing JH, Ringgaard S, et al. Experimental articular cartilage repair in the Göttingen minipig: the influence of multiple defects per knee. J Exp Orthop. 2015;2:13. doi:10.1186/s40634-015-0031-3.